

INTERACTIONS OF CHITOSAN/GENIPIN HYDROGELS DURING DRUG DELIVERY: A QSPR APPROACH

Nancy L. Delgadillo-Armendariz^a, Norma A. Rangel-Vazquez^{a,*}, Edgar A. Marquez-Brazon^{b,c} and Blanca Rojas-De Gascue^b^aDivisión de Estudios de Posgrado e Investigación, Instituto Tecnológico de Aguascalientes, Ave. López Mateos #1801 Ote. Col. Fracc. Bona Gens CP 20256, Aguascalientes, Ags. México^bUniversidad de Oriente, Instituto de Investigaciones en Biomedicina y Ciencias Aplicadas, "Dra. Susan Tai", IIBCA-UDO, Apdo. Postal 245, Cumaná, Estado Sucre, Venezuela^cUniversidad de Oriente, Departamento de Química, Núcleo de Sucre, Apdo. Postal 245, Cumaná, Estado Sucre, Venezuela

Recebido em 10/04/2014; aceito em 27/06/2014; publicado na web em 05/09/2014

A hydrogel comprised of chitosan crosslinked using the low-toxicity crosslinker genipin was prepared, and the absorption of glibenclamide by the hydrogel was investigated. Optimized structures and their molecular electrostatic potentials were calculated using the AM1 method, and the results were used to evaluate the molecular interactions between the three compounds. The quantitative structure-property relationship model was also used to estimate the activity of the chemicals on the basis their molecular structures. In addition, theoretical Fourier transform infrared spectra were calculated to analyze the intermolecular interactions in the proposed system. Finally, the hydrophilicity of the hydrogel and its influence on the absorption process were also estimated.

Keywords: chitosan; genipin; glibenclamide; FTIR; QSPR modeling.

INTRODUCTION

The use of natural polymers (e.g., gelatin, chitosan, and silk proteins) for the development of hydrogels is gaining in importance owing to their inherent biocompatibility.¹ Hydrogels are high-water content materials prepared from crosslinked polymers that can provide sustained, local delivery of a variety of therapeutic agents. Use of the natural polymer chitosan as a scaffold material for hydrogels has been intensively investigated because of the polymer's biocompatibility, low toxicity, and biodegradability. Therefore, the advanced development of chitosan hydrogels has led to new drug delivery systems that release their payloads in response to varying environmental stimuli.^{2,3}

Chitosan (see Figure 1), the product of the *N*-deacetylation of chitin, has also received particular attention because it is produced as a waste product during crustacean (shrimp and crab) processing.⁴⁻⁸ In addition, it offers other advantages; chitosan can not only be used to control the release of active agents but also be prepared without the use of hazardous organic solvents because it is soluble in aqueous acidic solutions. Given the above-mentioned properties, chitosan is extensively used for the development of drug delivery systems.

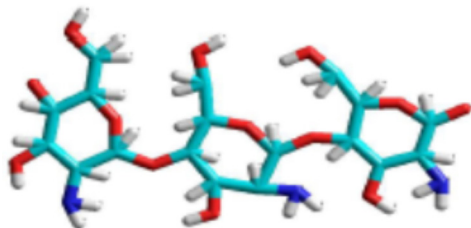


Figure 1. Chitosan structure (red: oxygen, white: hydrogen, blue: carbon and purple: nitrogen atoms)

Chitosan has been effectively used in drug delivery applications as hydrogel systems, drug conjugates, biodegradable release systems, and other components.^{9,10} Chitosan-based systems are used for the delivery of proteins/peptides, growth factors, anti-inflammatory

drugs, and antibiotics, as well as, in gene therapy and bioimaging applications.^{9,11,12}

The crosslinking of chitosan is considered a relevant approach for improving control of drug delivery. Among other reagents, glutaraldehyde and tripolyphosphate have been widely used to crosslink this biodegradable polymer. However, there are concerns over the toxicity of most of the investigated crosslinking agents, especially glutaraldehyde, which may reduce the biocompatibility of chitosan delivery systems. Therefore, there is a need for the development of crosslinking agents with low cytotoxicity.^{1,13}

Genipin, which is a natural, water-soluble, and bifunctional crosslinker¹⁴ (Figure 2) obtained from the fruits of *Gardenia jasminoides*¹, was selected for the study as a possible biocompatible crosslinker for chitosan. Genipin is an excellent natural crosslinker for proteins, collagen, gelatin, and chitosan. It has a low acute toxicity with an in vivo LD₅₀ of 382 mg/kg in mice and is 10,000 times less toxic than glutaraldehyde and degrades more slowly than glutaraldehyde and many other commonly used synthetic crosslinking reagents. Furthermore, genipin is also used as a regulating agent for drug delivery, as the raw material for gardenia blue pigment preparation, and as an intermediate for alkaloid synthesis.^{1,15-21}

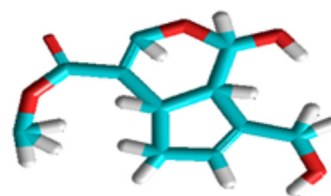


Figure 2. Genipin structure (red: oxygen, white: hydrogen and blue: carbon atoms)

Glibenclamide (see Figure 3), also known as glyburide, is an antidiabetic drug in the class of medications known as sulfonylureas, which are closely related to sulfa drugs. Sulfonylureas bind to ATP-dependent K⁺ channels in beta cells of the pancreas, depolarizing them and stimulating the release of Ca²⁺, which in turn stimulates insulin production.^{22,23}

*e-mail: normarangelvazquez201301@gmail.com

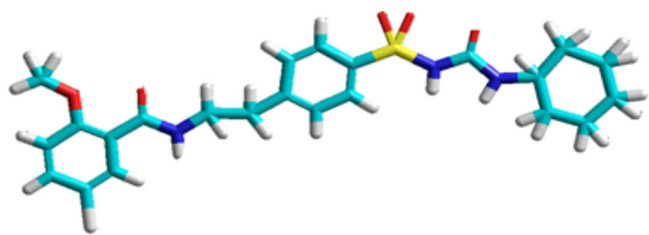


Figure 3. Glibenclamide structure (red: oxygen, white: hydrogen, blue: carbon, yellow: sulfur and purple: nitrogen atoms)

In this study, Fourier transform infrared (FTIR) spectroscopy was used to analyze the intermolecular interactions in the proposed system. As one of the ways to verify the obtained results, we apply the theoretical calculations by means of the computational chemistry tools.²⁴ Using the quantitative structure-property relationship (QSPR) model/method, we estimate the activity of the chemicals on the basis of only their molecular structure. Sorption of organic chemicals in soils or sediments is usually described by sorption coefficients.²⁵

In addition, the log P value of the hydrogel was determined as a measure of its hydrophobicity.²⁶ The log P value of a compound, which is the logarithm of its partition coefficient between *n*-octanol and water ($c_{\text{octanol}}/c_{\text{water}}$), is a well-established measure of the compound's hydrophilicity. Low hydrophilicities, and therefore high log P values, cause poor absorption or permeation. It has been shown that compounds must have a log P value less than 5 in order to have a reasonable probability of being well absorbed.²⁷ Typically, the log P value of a substance at pH 7.4 is considered as an index of the compound behavior in plasma.²⁸

Finally, the molecular electrostatic potential (MESP) was investigated using the Austin Method 1 (AM1) calculations. This method provides information about the regions in which intermolecular interactions occur between compounds.²⁹ The electrostatic potential is the energy of the interaction of a point positive charge (an electrophile) with the nuclei and electrons of a molecule. Negative electrostatic potentials indicate areas that are prone to electrophilic attack. The electrostatic potential can be mapped onto the electron density by using color to represent the value of the potential.³⁰

EXPERIMENTAL

The AM1 method was initially used to optimize the structures of the compounds investigated in the present study because it generates lower-energy structures, even when the initial structures are far away from the minimum structures. The Polak-Ribiere algorithm was used for mapping the energy barriers of the conformational transitions. For each structure, 5715 iterations, a level convergence of 0.001 kcal/mol/Å, and a line search of 0.1 were performed.

Structural parameters

The optimized structural parameters were used for the vibrational wavenumber calculations with AM1 method in order to characterize all the stationary points as minima. The structural parameters were calculated by selecting the Constrain bond and length options from the Build menu for the two methods of analysis.

FTIR

An infrared spectrum is commonly obtained by passing infrared electromagnetic radiation through a sample that possesses a permanent or induced dipole moment and determining what fractions of the incident radiation are absorbed at particular energies. The energy

of each peak in an absorption spectrum corresponds to the frequency of the vibration of part of the molecule, thus allowing qualitative identification of certain bond types in the sample.

The FTIR spectra were obtained by first selecting from the Compute menu, vibrational and rotational spectrum options; after this step, using the vibrational spectrum option, FTIR spectrum pattern is obtained for the two methods of analysis. The results of the analyses for the optimized structures for chitosan, genipin, and glibenclamide obtained using the AM1 method are listed in Tables 1–3, respectively.

Table 1. FTIR results of chitosan

Assignment	Experimental (Frequencies cm ⁻¹) ²⁷⁻²⁹	AM1 (Frequencies cm ⁻¹)
CH (CH ₂ -OH) stretching	-----	4374
OH and CH (CH ₂ -OH)	3550	3676
CH (CH ₂ -OH) stretching	-----	3512
NH	3314	-----
OH (CH ₂ -OH)	-----	3300
C-N	1360-1080	2041
C-C	-----	1909
NH ₂	1580	-----
C-O (chitosan ring)	1150	1489

Table 2. FTIR results of genipin

Assignment	Experimental (Frequencies cm ⁻¹) ³⁰⁻³²	AM1 (Frequencies cm ⁻¹)
OH stretching	-----	6052
CH ₂ asymmetric stretching	-----	4694, 4530
CH stretching (ring)	3745	4091, 3885
C=C	3398, 3245	3354
CH ₂ (scissoring)	3100	3039
C-C, C-O	2520	2680, 2571
C-C, C-O, CH	1681, 1622, 1105	1663, 1038
CH ₃ , CH ₂	1443	1405
C-O-C	830, 835	818
C-O-C (out of plane)	773	755

Table 3. FTIR results of glibenclamide

Assignment	Experimental (Frequencies cm ⁻¹) ³³⁻³⁵	AM1 (Frequencies cm ⁻¹)
NH asymmetric stretching	-----	5583
CH asymmetric stretching	-----	5007
CH ₂ stretching	-----	4511
CH ₃ (O-CH ₃)	3591	4028
NH (amide)	3367, 3311, 1713	3314
CH=CH	3035	3529
C=C (ring)	1591	2830
C=C, S=O	2412	2474
C=O	1652, 1618	1720, 1715
S=O ₂	1341-1332, 1158	1316
C-C, C-N, C-O	1995, 1334, 1154, 1090, 1018, 924, 793	1332, 1124, 1028, 569

Electrostatic potential

After obtaining the Gibbs free energy for the optimized geometries using the AM1 method, two-dimensional contour diagrams of the electrostatic potentials surrounding the three molecules, their total electron densities and spin densities, their molecular orbitals, and the electron densities of the individual orbitals were plotted.

HyperChem software displays the electrostatic potential as a contour plot when the appropriate option in the Contour Plot dialog box is selected. Atomic charges indicate where large negative values (sites for electrophilic attack) are likely to occur. However, the largest negative value for the electrostatic potential is not necessarily adjacent to the atom with the largest negative charge.³¹

RESULTS AND DISCUSSION

Structural parameters

The thermodynamic data obtained are listed in Table 4. The Gibbs free energy value (-947.998 kcal/mol) indicates that the crosslinking reaction involves crosslinking of two free amino groups in chitosan with one molecule of genipin (see Figure 4).^{17,18} Nucleophilic attack by the primary amine occurs at the carbon atom in genipin, while the secondary amine attacks the aldehyde group.²¹

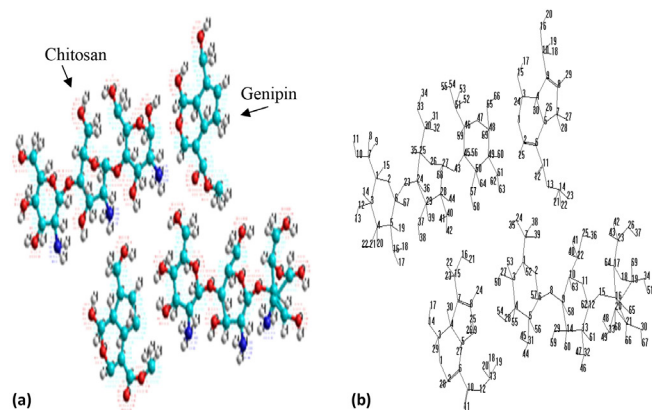


Figure 4. Structure of chitosan/genipin using computational chemistry

QSPR methodology is one of the most powerful tools for describing the relationship between the biological activity and physicochemical characteristics of a molecule. Diffusion is also influenced by the nature of the crosslinker. In addition, the porosity, water uptake, and swelling of hydrogels are influenced by the chemical nature and length of the bridging units of the crosslinker.

Table 4. QSPR properties results

Property	Chitosan/Genipin	Chitosan/Genipin-Glibenclamide
ΔG (kcal/mol)	- 947.998	- 243.08
Mass (amu)	1455.43	2442.44
Surface area (\AA^2)	1798.11	2910.84
Volume (\AA^3)	3507.66	5860.58
Log P	- 22.15	- 46.33

Swelling and diffusion in hydrogels are also influenced by the hydrophilicity of the crosslinked polymer.³² Therefore, the Log P value for chitosan/genipin was calculated and found to be -22.15 . This value represents the hydrophilic property of the substance and is

considered to be an indicator of the ability of the hydrogel to absorb molecules.³³ In hydrogels formed by chitosan crosslinked with itself, release is largely controlled by the crosslinking density; consequently, the higher the crosslinking density, the lower the release rate.

However, other system parameters, such as drug concentration, often play a major role. To our knowledge, there are no examples of hydrogels formed by chitosan crosslinked with itself that exhibit pH-sensitive swelling.

Indeed, the numerous inter-chain interactions formed by crosslinking inhibit swelling because most of the amino groups of chitosan react with the crosslinker. Such systems do not present a release profile that can be further modulated after administration; for example, drug release cannot be targeted in the gastro-intestinal tract, which limits their range of application.^{5,32}

Table 4 shows the thermodynamic results of glibenclamide absorption process; here the Gibbs free energy value -243.08 kcal/mol is spontaneous because of the formation of hydrogen bonds between the carbonyl groups of glibenclamide and NH groups of chitosan. Nucleophilic attack of the amino group of chitosan at the carbonyl of the genipin leads to formation of a stable bond (amide), and an oxygen atom in genipin is replaced by a nitrogen atom from chitosan (see Figure 5).³⁴

Figure 5 shows that the title system (chitosan-genipin/glibenclamide) is not planar, and based on observations, deformation of the ring structure depends on the nature of the substituents (OH, NH_2 , and $\text{CH}_2\text{-CH}_2$). Figure 5 shows the results of the computational analysis to determine the optimized geometries for chitosan/genipin and chitosan (genipin)/glibenclamide. Their molecular structures as well as the numbering of their atoms are also shown in the figure.

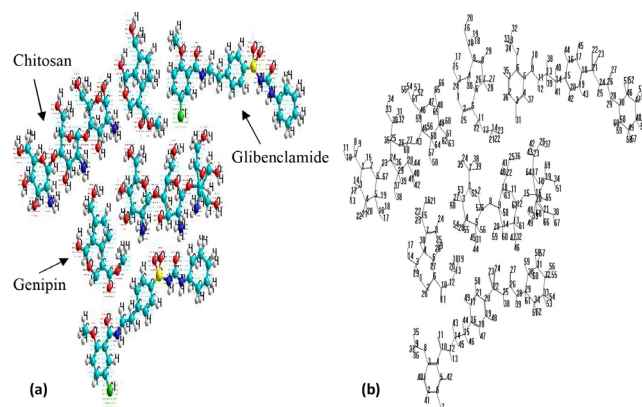


Figure 5. Structure of (chitosan (genipin)/glibenclamide) using computational chemistry

The optimized structural parameters for chitosan, chitosan crosslinked with genipin, and the chitosan/genipin hydrogel with absorbed glibenclamide are listed in Tables 5–7, respectively, in accordance with the atom numbering scheme given in Figures 4 and 5. The title system (chitosan-genipin/glibenclamide) is not planar, and based on observations, deformation of the ring structure depends on the nature of the substituents (OH, NH_2 , and $\text{CH}_2\text{-CH}_2$). Therefore, we could compare the calculation results given in Tables 5–7 with experimental data. As discussed in the previous literature, several authors have explained the changes in frequency or bond length of the C–H bond upon substitution due to a change in the charge distribution on the carbon atom of the ring.³¹ The substituents may either be electron withdrawing (Cl, Br, F) or electron donating (CH_3 , C_2H_5).

The carbon atoms are bonded to hydrogen atoms via σ bonds, and substitution of a hydrogen atom for a halogen atom on the benzene

Table 5. Structural parameters calculated for chitosan crosslinking with genipin using AM1 method

Bond	Bond Length (Å)	Bond	Bond Length (Å)	Bond	Bond Length (Å)
C1-O2	1.4381	C48-C49	1.5817	C1-C3-C4	127.634
C1-C3	1.5904	C49-C50	1.7053	C3-C4-C5	113.850
C3-C4	1.6297	C50-C45	1.6117	C4-C5-C6	115.739
C4-C5	1.5601	O1-C2	1.4576	C5-C6-O2	123.671
C5-C6	1.5321	C2=C6	1.4415	C6-O2-C1	132.400
C6-O2	1.4098	C6-C5	1.6407	C1-C3-C7	121.190
C6-O23	1.4589	C5-C4	1.6765	C1-O2-H15	42.624
O23-C24	1.4962	C4-C3	1.6015	C3-C4-O12	109.238
C24-C25	1.7340	C3-O1	1.5114	C3-C4-O21	114.163
C25-O26	1.4315	C4-C7	1.7063	C5-N16-H19	57.759
O26-C27	1.4199	C7=C8	1.4761	C6-O2-O23	84.355
C27-C28	1.7312	C8-C9	1.6468	C6-O23-C24	145.82
C28-C29	1.7856	C9-C5	1.5974	C24-C25-O26	74.147
C29-C24	1.7101	C6-C10	1.5198	C25-O26-C27	154.861
C27-O43	1.4325	C10-O12	1.3882	C28-C27-O26	84.041
O43-C45	1.4829	O12-C13	1.4401	C27-C28-C29	117.163
C45-C46	1.6543	C7-C15	1.5559	C28-C29-C24	111.111
C46-O47	1.5741	C15-O16	1.4162	C24-C25-C29	128.399
O47-C48	1.5016	C1-C2-C3	106.706	C27-O43-C45	124.727
C27-O43-C45	124.727	C45-C49-C50	117.553	C6=C2-O1	104.633
C28-C29-N40	102.693	C45-C46-C50	121.814	C7-C4-C5	97.657
C28-C29-N40	102.693	C45-C46-C50	121.814	C7-C4-C5	97.657
C25-C26-C30	96.463	O1-C2-C3	147.037	C4-C7=C8	109.055
C45-C46-O47	106.214	O1-C2-C4	107.247	C7=C8-C9	118.073
C46-O47-C48	143.331	C3-C4-C5	116.823	C5-C9-C8	96.801
O47-C48-C49	109.347	C6-C4-C5	116.932	C5-C6-C10	126.041
C48-C49-C50	121.741	C5-C6=C2	127.328	C12-C6-C10	136.259

ring reduces the electronic density at the carbon atom owing to an induction effect. The ring carbon atoms exhibit a larger attraction for the valence electron cloud of the remaining hydrogen atoms, resulting

Table 6. Bond length calculated for chitosan (crosslinking with genipin)/glibenclamide using AM1 method

Bond	Bond Length (Å)	Bond	Bond Length (Å)	Bond	Bond Length (Å)
C1-C3	1.5904	C4-C3	1.6290	O26-C27	1.4198
C1-O2	1.4392	C6-O23	1.4606	C27-C28	1.7307
O2-C6	1.4106	O23-C24	1.4979	C28-C29	1.7857
C6-C5	1.5326	C24-C25	1.7343	C29-C24	1.7105
C5-C4	1.5599	C25-O26	1.4315	C27-O43	1.4325
O43-C45	1.4828	C10-N12	1.3458	C6-C10	1.5195
C45-C46	1.6548	N12-C14	1.4551	C7-C15	1.5556
C46-O47	1.5737	C14-C15	1.6129	C31-C32	1.6139
O47-C48	1.5008	C15-C16	1.5797	C32-C33	1.5749
C48-C49	1.5816	C16-C17	1.5147	C33-C34	1.6242
C49-C50	1.7053	C17=C21	1.3415	C34-C29	1.7610
C50-C45	1.6717	C21-C20	1.4668	C26-O27	1.2279
O1-C3	1.5116	C20=C19	1.3411	S22-O23	1.5798
C3-C4	1.6016	C19-C18	1.4664	S22-O24	1.5794
C4-C5	1.6762	C18=C16	1.3563	C10-O11	1.2316
C5-C6	1.6404	C20-S22	1.7650	N28-C29	1.4657
C6=C2	1.4415	S22-N25	1.7177	C29-C30	1.5879
C2-O1	1.4579	N25-C26	1.3478	C30-C31	1.6051
C4-C7	1.7066	C26-N28	1.3436	C9-C5	1.5969
C7=C8	1.4762	C8-C9	1.6465		

in an increase in the C–H force constant and a decrease in the corresponding bond lengths. The reverse holds true for substitution with electron donating groups.

The actual change in the C–H bond lengths is influenced by the combined effects of the inductive–mesmeric interaction and the electric dipole field of the polar substituent. The calculated geometric parameters can be used as the foundation for calculating other parameters for the compound.³⁵

FTIR

The calculated FTIR results for chitosan/genipin and chitosan (crosslinked with genipin)/glibenclamide are presented in Table 8. The second column indicates the absorption bands at 2320 and 1097 cm^{-1} , which clearly appeared after crosslinking with genipin. The peak at 1097 cm^{-1} represents the C–N stretching vibration for the tertiary nitrogen atom formed from the reaction of the lysine with genipin, while the band at 2320 cm^{-1} was assigned to C–C, C–H, C–O, and C–N bonds that formed following crosslinking. Moreover, the adsorption band that appeared at 1236 cm^{-1} (amide III) represents a mixed CO–N/N–H vibration mode, and the peak at 813 cm^{-1} is a characteristic absorption band for the C–H stretching vibration associated with the heterocyclic ring of the product.

An amine group in the chitosan macromolecule undergoes nucleophilic attack at the C–OH group of genipin, resulting in the formation of a new covalent bond between the aldehyde group and the secondary amine and formation of a double bond at the carbon in the ortho-position.^{16,17,36–38} One of the most important changes is evident in the reduction of the carbonyl group of the genipin, which reacts with the primary amine in chitosan to form an amide, which

Table 7. Angle calculated for chitosan (crosslinking with genipin)/glibenclamide using AM1 method

Bond	Angle (°)	Bond	Angle (°)	Bond	Angle (°)
C1-C3-C4	127.626	C45-O47-C46	106.193	C6-C10-O12	136.273
C5-C3-C4	113.831	C45-C51-C46	135.376	C10-O12-C13	146.014
C6-C5-C4	115.859	C45-O47-C48	143.381	C9-C5-C6	124.608
O2-C5-C6	123.559	C49-O47-C48	109.344	C1=C2-C6	119.726
C1-O2-C6	132.357	C49-C50-C48	121.732	C2-C6=C5	119.633
C1-C3-O2	106.768	C49-C50-C45	117.545	C6=C5-C4	121.828
C1-C3-C7	121.067	C46-C50-C45	121.806	C5-C4=C3	118.351
O12-C3-C4	109.22	C50-C49-N61	106.1840	C4=C3-C1	119.103
O21-C3-C4	114.184	O1-C3-C4	107.2720	C1-C3-O8	121.394
C5-C6-N16	147.176	C3-C4-C5	116.783	C3-O8-C9	133.702
C6-O2-O23	84.6643	C4-C5-C6	116.972	C5-C4-C10	117.572
C24-O23-C25	109.381	C5-C6=C2	127.341	C3-C1=C2	121.358
C24-C25-O26	74.1901	C6=C2-O1	104.610	C4-C10-N12	120.165
C25-C26-C27	154.839	C2-O1-C3	147.022	C4-C10=O11	120.411
C28-C26-C27	84.0271	O1-C3-O14	132.731	O11=C10-N12	119.425
C27-C28-C29	117.165	C4-C5-C7	97.6437	C10-N12-C14	124.203
C24-C28-C29	111.158	C4-C7=C8	109.065	N12-C14-C15	137.288
C24-C29-O37	102.782	C7=C8-C9	118.035	C14-C15-C16	145.455
C27-C28-N40	140.123	C8-C9-C5	96.8362	C15-C16=C18	118.951
C27-C28-O43	84.0492	C9-C5-C4	118.42	C15-C16-C17	127.566
C25-C30-O26	96.3597	C4-C7-C15	133.485	C16-C17=C21	123.344
C27-O43-C45	124.622	C7-C15-O16	126.308	C17=C21-C20	120.522
C45-O43-C46	132.147	C5-C6-C10	125.969	C21-C20=C19	117.485
C20=C19-C18	121.978	C18=C16-C17	113.483	C33-C34-C29	126.013
C19-C18=C16	123.188	C28-C29-C30	121.280	N28-C26=O27	122.574
C20-S22-N25	128.431	C29-C30-C31	131.325	N25-C26=O27	124.259
S22-N25-C26	132.168	C30-C31-C32	122.219	O24=S22-N25	97.0564
N25-C26-N28	113.167	C31-C32-C33	113.669	O23=S22=O24	40.1588
C26-N28-C29	130.906	C32-C33-C34	122.978	C20-S22=O23	94.3538
C19=C20-S22	117.351				

is indicated by the growth of the absorption band at 1630 cm^{-1} in the FTIR spectrum of the hydrogel.

As a consequence of these two main reactions, the intensity of the absorption band for the amino groups at 3597 cm^{-1} is drastically reduced in the spectrum of the hydrogel.³⁶⁻⁴⁰

The third column in Table 8 lists the absorption bands that appeared after the absorption of glibenclamide by the chitosan/genipin crosslinked hydrogel. These peaks include a characteristic amide band at 3407 cm^{-1} and peaks for SO and SO_2 stretching vibrations at 2683 and 1369 cm^{-1} , respectively. The site of interaction on glibenclamide is likely the C=O group, which would also affect the NH vibration.³⁸

The absorption peaks observed at 2412 and 793 cm^{-1} are associated with C–C, CH, C–O, and OH bending vibrations, while the absorption bands at 1955 , 1334 , 1090 , and 924 cm^{-1} are due to the C–C and C–O bonds in the chitosan crosslinked with genipin.⁴¹ The new broad peak that appeared near 1415 cm^{-1} after crosslinking with genipin is associated with the ring-stretching vibrations of the heterocyclic amine. In addition, the C–N stretching of amide III at 1233 cm^{-1} shifted to 1260 cm^{-1} after crosslinking with genipin, while the peak at 1740 cm^{-1} , which corresponds to the carboxylic groups in the electrospun chitosan fibers, disappeared in the genipin-crosslinked chitosan.³⁹

Electrostatic potential

The MESP values (Figure 6) ranged from -0.075 to 0.607 eV and 0.065 to 0.718 eV for the crosslinking of chitosan with genipin and glibenclamide absorption by the crosslinked hydrogel, respectively.

Table 8. FTIR results using computational chemistry

Assignments / Wavenumber (cm^{-1})	Chitosan/Genipin	Chitosan(Genipin)-Glibenclamide
N–H and CH stretching	3859	4412
OH stretching	-----	4412
CH ₂ scissoring (genipin)	3597	3460
NH (glibenclamide)	-----	3407
CH ₂ scissoring (glibenclamide)	-----	3298
C=C (glibenclamide)	-----	2884
CH=CH, C=O, S=O (glibenclamide)	-----	2683
NH ₂ asym stretching and OH stretching	3458, 3295	-----
C–C, CH, C–O and OH (absorption of glibenclamide)	-----	2412, 793
C–O, C–C, C–H (genipin)	3089, 1441, 721	2320
C–C, C–O, C–N (absorption of glibenclamide)	2884, 2683, 1952	1955, 1334, 1090, 924
C–C, C–H, C–O, C–N (chitosan and genipin)	2320	-----
S=O ₂	-----	1369
C=O (Genipin-amide group)	1630	1715
CO–N, N–H	1236	1235
C–O, C–N, C–C (chitosan and genipin)	813	724

The negative regions appeared near the OH groups (C–OH bonds) in the crosslinked chitosan.

The absorption of glibenclamide by the chitosan crosslinked with genipin mainly involved the formation of hydrogen bonds between the CH₂OH and CH groups. Figure 7 shows the structure of the genipin-crosslinked chitosan with absorbed glibenclamide.

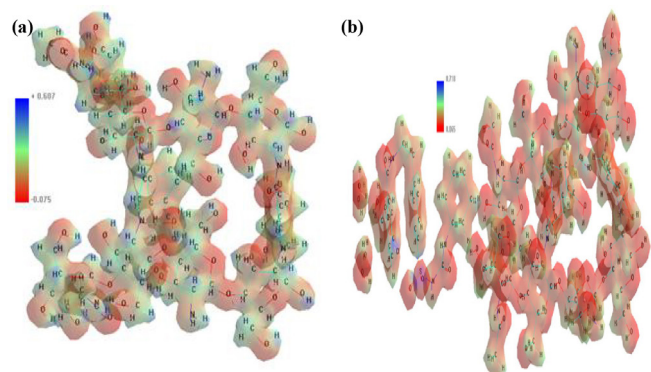


Figure 6. MESP, from which (a) chitosan/genipin and (b) chitosan (genipin)/glibenclamide, respectively

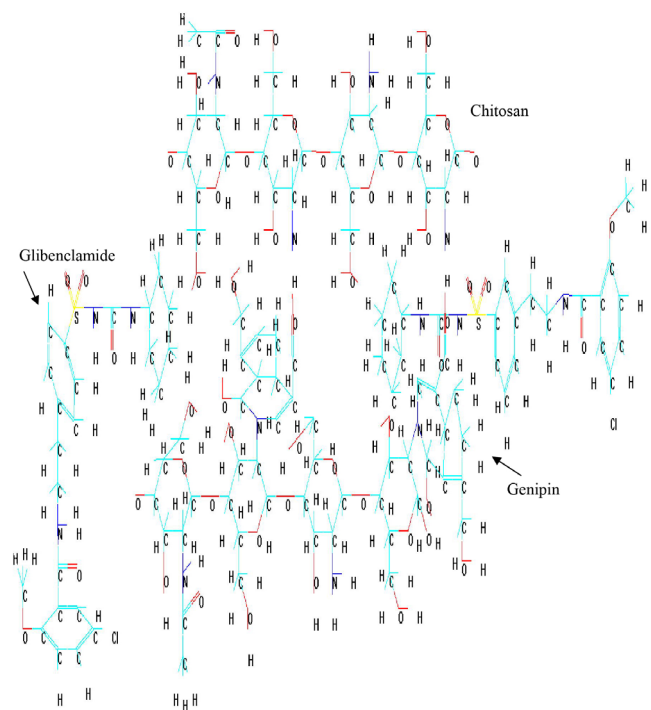


Figure 7. Structure of chitosan (genipin)/glibenclamide absorption

CONCLUSIONS

Genipin, a natural crosslinking agent, reacts with compounds containing primary amine groups, such as chitosan, to form covalently crosslinked networks. In the case of chitosan, genipin reacts with the free amino groups present in the glucosamine units. The results of this study support the relevance of genipin as a valuable natural, nontoxic, crosslinking agent for controlled drug release in drug delivery systems based on chitosan.

The negative log P values for the crosslinked chitosan indicated that absorption properties of the hydrogel are dominated by its hydrophilic character and that absorption plays an important role in both glibenclamide absorption partitioning and receptor-binding. It

was also shown that genipin changes the hydrophilicity of chitosan. FTIR results revealed that secondary amide linkages are formed via the reaction of genipin ester groups with chitosan amino groups, yielding a polymeric network structure. The MESP values indicated that the nucleophilic and electrophilic regions mainly involved the NH/C–OH and C=O bonds, respectively.

REFERENCES

- Thakur, G.; Mitra, A.; Rousseau, D.; Basak, A.; Sarkar, S.; Pal, K.; *J. Mater. Sci.: Mater. Med.* **2011**, *22*, 115.
- Bhattacharai, N.; Gunn, J.; Zhang, M.; *Adv. Drug Delivery Rev.* **2010**, *62*, 83.
- Muzzarelli, R. A.; *Carbohydr. Polym.* **2009**, *77*, 1.
- Wu, C. S.; *Polymer* **2005**, *46*, 147.
- Berger, J.; Reist, M.; Mayer, J. M.; Felt, O.; Peppas, N. A.; Gurny, R.; *Eur. J. Pharm. Biopharm.* **2004**, *57*, 19.
- Diaconu, M.; Tache, A.; Victoria, S. A.; Gatea, F.; Litescu, S.; Radu, G.; *UPB Scientific Bulletin, Series B: Chemistry and Materials Science* **2010**, *72*, 115.
- Patel, M.; Ravi, R.; Patel, J.; Patel, K.; *J. Pharm. Pharm. Sci.* **2010**, *13*, 536.
- Sailaja, A. K.; Amareshwar, P.; Chakravarty, P.; *J. Pharm. Biol. Chem. Sci.* **2010**, *1*, 474.
- Dash, M.; Chiellini, F.; Ottenbrite, R. M.; Chiellini, E.; *Prog. Polym. Sci.* **2011**, *36*, 981.
- Grolik, M.; Szczubiałka, K.; Wowra, B.; Dobrowolski, D.; Orzechowska-Wylęgała, B.; Wylęgała, E.; Nowakowska, M.; *J. Mater. Sci.: Mater. Med.* **2012**, *23*, 1991.
- Bansal, V.; Sharma, P. K.; Sharma, N.; Pal, O. P.; Malviya, R.; *Adv. Biol. Res.* **2011**, *5*, 28.
- Bhattacharai, N.; Gunn, J.; Zhang, M.; *Adv. Drug Delivery Rev.* **2010**, *62*, 83.
- Harris, R.; Lecumberri, E.; Heras, A.; *Mar. Drugs* **2010**, *8*, 1750.
- Karnchanajindanun, J.; Srisa-Ard, M.; Srihanam, P.; Baimark, Y.; *Nat. Sci.* **2010**, *2*, 1061.
- Zhang, C. Y.; Parton, L. E.; Ye, C. P.; Krauss, S.; Shen, R.; Lin, C. T.; Porco, J. A.; *Cell Metab.* **2006**, *3*, 417.
- Park, J. E.; Lee, Y.; Kim, H. G.; Hahn, T. R.; Paik, Y. S.; *J. Agric. Food Chem.* **2002**, *50*, 6511.
- Wang, L.; Wang, Y.; Qu, J.; Hu, Y.; You, R.; Li, M.; *J. Biomater. Nanobiotechnol.* **2013**, *4*, 213.
- Imsoambut, T.; Srisuwan, Y.; Srihanam, P.; Baimark, Y.; *Powder Technol.* **2010**, *203*, 603.
- Silva, S. S.; Maniglio, D.; Motta, A.; Mano, J. F.; Reis, R. L.; Migliaresi, *Macromol. Biosci.* **2008**, *8*, 1.
- Taylor, M.; Ding, K.; Brown, E.; *J. Am. Leather Chem. Assoc.* **2009**, *1*.
- Yoo, J. S.; Kim, Y. J.; Kim, S. H.; Choi, S. H.; *The Korean Journal of Thoracic and Cardiovascular Surgery* **2011**, *44*, 197.
- Serrano-Martín, X.; Payares, G.; Mendoza-León, A.; *Antimicrob. Agents Chemother.* **2006**, *50*, 4214.
- <http://www.scbt.com/es/datasheet-200982-glyburide-glibenclamide.html>, accessed July, 2014.
- Mon, J.; Flury, M.; Harsh, J. B.; *J. Hydrol.* **2006**, *316*, 84.
- Zhang, X. H.; Zhan, Y. H.; Chen, D.; Wang, F.; Wang, L. Y.; *Dyes Pigm.* **2012**, *93*, 1408.
- <http://www.molinspiration.com/services/logp.html>, accessed July, 2014.
- <http://www.organic-chemistry.org/prog/peo/cLogP.html>, accessed July, 2014.
- <http://www.admescope.com/learn-adme/physicochemical-properties/lipophilicity-logd-logp.html>, accessed July, 2014.
- Glish, L.; Hanks, T. W.; *J. Chem. Educ.* **2001**, *84*, 2001.
- <http://www.prudencepharma.com/Glibenclamide.html>, accessed July, 2014.

31. Dash, S. K.; Khan, A. S.; Das, S. R.; Padhan, A.; Rout, D.; Behera, B. C.; *Int. J. Pharm. Sci. Res.* **2012**, 3, 1433.
32. Rangel-Vázquez, N. A.; Rodríguez-Felix, F.; *Computational Chemistry Applied in the Analyses of Chitosan/Polyvinylpyrrolidone/Mimosa Tenuiflora*, Science Publishing Group: Hong Kong, 2013, cap. 2, pp. 25-26.
33. Hwang, Y. J.; Krasieva, T.; Lyubovitsky, J.; *ACS Appl. Mater. Interfaces* **2011**, 3, 2579
34. Santoni, N.; Matos, M.; Müller-Karger, C.; Nicola, H.; Sabino, M.; Müller, A.; *Revista Iberoamericana de Polímeros* **2008**, 9, 326.
35. Gunasekaran, S.; Rajalakshmi, K.; Kumaresan, S.; *Spectrochim. Acta, Part A* **2013**, 112, 351.
36. Lertsutthiwong, P.; Noomun, K.; Khunthon, S.; Limpanart, S.; *Prog. Nat. Sci.: Mater. Int.* **2012**, 22, 502.
37. Yao, C. H.; Liu, B. S.; Chang, C. J.; Hsu, S. H.; Chen, Y. S.; *Mater. Chem. Phys.* **2004**, 83, 204.
38. Levinton-Shamuilov, G.; Cohen, Y.; Azoury, M.; Chaikovsky, A.; *J. Forensic Sci.* **2005**, 50, 1367.
39. Bahri-Najafi, R.; Tavakoli, N.; Senemar, M.; Peikanpour, M.; *Res. Pharm. Sci.* **2014**, 9, 213.
40. Rodríguez, R.; *Tesis de Licenciatura*, Universidad de Oriente, Cumaná, Venezuela, 2010.
41. Mirzaei, E.; Faridi-Majidi, R.; Shokrgozar, M. A.; Paskiabi, F. A.; *Nanomed. J.* **2014**, 1, 137.